

## **SILVER NANOPARTICLES SINTERING AT LOW TEMPERATURE ON A COPPER SUBSTRATE: IN SITU CHARACTERISATION UNDER INERT ATMOSPHERE AND AIR**

**J. Sopousek<sup>#,\*</sup>, J. Bursik<sup>\*\*</sup>, J. Zalesak<sup>\*</sup>, Z. Pesina<sup>\*\*\*</sup>**

<sup>\*</sup>Department of Chemistry, Faculty of Science, Masaryk University,  
Kotlarska 2, Brno, Czech Republic

<sup>\*\*</sup>Institute of Physics of Materials, AS CR, Zizkova 22, 616 62 Brno, Czech Republic

<sup>\*\*\*</sup>Institute of Material Science and Engineering, Faculty of Mechanical Engineering, Brno  
University of Technology, Technická 2896/2, 616 69 Brno, Czech Republic

*(Received 18 July 2011; accepted 12 October 2011)*

---

### **Abstract**

*Silver nanoparticles (Ag-NPs) were prepared by wet synthesis. The Ag-NPs suspension and the copper substrate plate were used for a preparation of substrate-nanoparticle-substrate samples. The sandwich like samples Cu/Ag/Cu were prepared and investigated in-situ at the isothermal external conditions (IEC) and inside apparatus for simultaneous thermal analysis STA409. The in-situ results of the electrical resistance were recorded during the Cu/Ag/Cu (IEC) sample preparation and heat treatment. Thermal effects of the Ag-NPs sintering between copper substrates were measured by differential scanning calorimetry (DSC) under different atmospheres. The prepared Cu/Ag/Cu sandwich samples were characterised by means of both optical and electron microscopy. The process of the low temperature sintering of the Ag-NPs was monitored using both thermogravimetry (TG) and DSC technique inside calorimeter under inert gas and under synthetic air. The exothermic heat effect of nanosilver sintering was evaluated.*

*Keywords: Silver, copper, DSC, electrical resistance, heat of sintering.*

### **1. Introduction**

Metal and alloy nanoparticles are interesting objects, which have potential to achieve functions that can be hardly realised by use of conventional bulk materials. The

---

<sup>#</sup> Corresponding author: [sopousek@chemi.muni.cz](mailto:sopousek@chemi.muni.cz)

main reason of the difference between behaviour of nanomaterial and bulk material is a high surface-to-volume ratio of nanomaterial. Nanoparticles have low value of cohesive energy [1] and high surface energy. It leads to a natural nanoparticle preference for aggregation. This property can be an advantage as well as disadvantageous. The pure metals and alloy nanoparticles are used or considered for new applications and special technologies (flexible displays, electronic skins, solar cells, conductive printing, etc.).

Another specific property is that melting point of metallic nanoparticles depends on the nanoparticle size [2]. This effect can be observed in systems with protective shell where the nanoparticles do not interact with each other [3, 4]. Otherwise, nanoparticles aggregate easily. The metal and alloy nanopowders are promising materials for the conductive bonding in electronic industry and this technology seems to be one of the alternatives of lead-free soldering. The exploitation of the metal nanoparticles for conductive bonding and joining offers also another interesting aspect that manufacturing temperature can be lower than subsequent operational use.

The silver nanoparticles (Ag-NPs) are often used for different technologies including antibacterial applications, photocatalysis, conductive ink jet printing, etc. Remarkable application is also the preparation of conductive plates (PCB) using an office-printing technology [4]. The Ag nanopowder production over the world is high [5]. The nanosilver represents also an interesting model material, which can be used for study of the solid-phase

nanosintering. The sintering was observed also below temperature 380°C (which is 0.42  $T_m$  of bulk silver). This enables the conductive bonding of the substrates for electronics at low temperature range [6]. The cohesion and strength of the copper substrate/nanosilver conductive joint are also objects of interest [7, 8].

The preparation of the conductive joint between two materials at low temperature by use of the metal nanoparticles (Me-NPs) seems to be very attractive technology for removing lead-solders from industrial applications but this process is not yet optimal. The Cu substrate/Ag-NPs system was object of this in-situ study in order to attain more detailed information about the phenomenon of the low-temperature nanosintering.

### **3. Experimental**

Ag-NPs were prepared by wet synthesis [9]. The obtained Ag-NPs were stored and manipulated as a suspension of Ag-NPs in toluene. Share of Ag-NPs was high - about 54 wt% (i.e. cca 9 vol%).

The Ag-NPs suspension and the copper substrate plate were used for a preparation of sandwich like samples: Cu / Ag-NPs / Cu. Purity of copper plate was 99.9wt%. The copper surface was always deprived of copper oxide before each experiment. The experimental procedure was such that few droplets of the Ag-NP suspension were put between two copper substrate disks (diameter 5.5 mm, height 0.127 mm) made from the Cu-plate. The Cu/Ag-NPs/Cu sandwich was created. The sandwich was inserted between two electrodes, which were

arranged inside alumina crucible. One electrode had needle shape with a thermocouple inside. This arrangement was put into preheated furnace (200, 250, 300, or 350°C, air) and both electrical resistance and immediate temperature measurements in situ were performed in course of the temperature equilibrating of the sandwich. The sandwich was pulled out and cooled down on air after 1.5 hr of heat exposure. Well-joined Cu/Ag/Cu sandwich samples were obtained. These sandwich samples prepared at the isothermal external conditions Cu/Ag/Cu (IEC) were used for further investigation.

The Cu/Ag(s)/Cu (IEC) sandwich samples were cut perpendicularly to the layer of silver (about in the middle of the sample). The light metallography was applied to investigate the sample morphology. All samples were also examined by electron microscopy (Scanning Electron Microscope (SEM), TESCAN LYRA3 FEG-SEMxFIB and JEOL JSM 6460) with Oxford Instruments INCA Energy analyzer (EDX). The chemical composition changes at the interfaces of Cu/Ag were observed using EDX microanalysis. Moreover, nanoindentation tests were also carried out [10].

Apparatus for simultaneous thermal analysis STA409 (Nezsch company) was also used for preparing sandwich samples. Each sample was prepared by dripping of the Ag-NPs suspension between two Cu substrates. The sandwich was closed in a small alumina crucible with lid and put in STA409 apparatus. The device was closed and the sample heated up. Thermal effects were measured by differential scanning calorimetry (DSC) under given atmosphere.

The background (DSC base line) was measured using a reference made of two Cu discs. The speeds of heating and cooling were 10K/min. Thus it was possible to monitor the thermal effects accompanying the repeated heating and cooling of sandwiches under different carrying gases (6N argon, 4.7 nitrogen, synthetic air). The prepared Cu/Ag/Cu (DSC) sandwiches were subjected to the same analysis as the Cu/Ag/Cu (IEC) samples.

### 3. Results

The suspension of the synthesized Ag-NPs was characterised by means of the high-resolution electron microscopy (HRTEM). The solvent phase was evaporated and the Ag nanoparticles were consequently investigated on carbon replicas. The majority fraction of the nano-particles was sized approx.  $20\pm 5$  nm (see Fig. 1.). The fraction of the nano particles with dimensions of about (120-200) nm was detected. The HRTEM showed that the particles have a very regular lattice of the fcc silver phase. The surface oxidation of the silver nanoparticles has not been observed.

The in-situ results of the temperature measurements and electrical resistance were recorded during the Cu/Ag/Cu (IEC) sample preparation. The obtained records are shown in Fig. 2. The measurements were performed at the different preheating temperatures of the furnace (200-350)°C. The temperature record of the each sample goes from room temperature to the furnace temperature. Heating rate of samples at 110 °C was around (15-5)°C / min. It can be distinguished in the first stage (time around

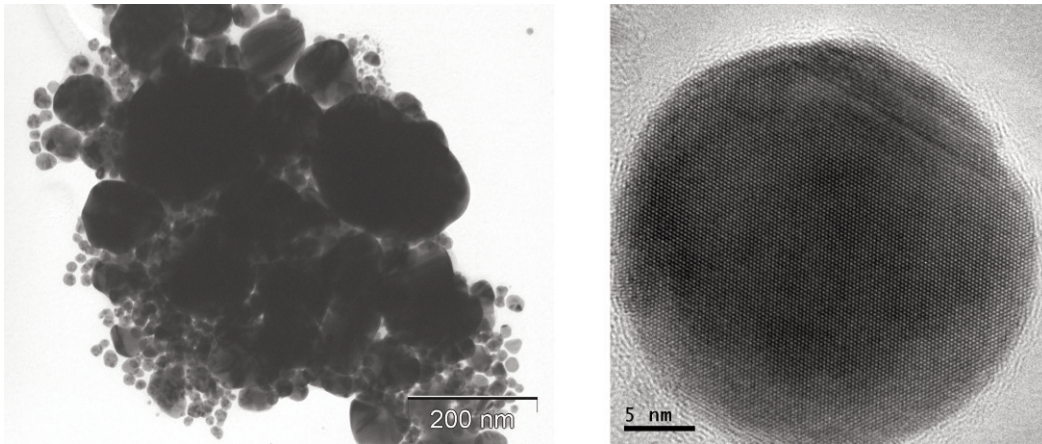


Fig.1. Silver nanoparticles. Overview (left, TEM) and detail (right, HRTEM). Silver fcc lattice ( $a=0.424\text{nm}$ , tabulated value for Ag:  $0.40862\text{nm}$ ).

(0-5 min) of heat treatments, that the electrical resistance of the samples increases when temperature goes from  $25^\circ\text{C}$  to approx.  $100^\circ\text{C}$ . In the second stage, which can be observed for all samples, an exponential fall in electrical resistance was observed. The third stage, an increasing of the electrical resistance from value close to zero to approx.  $0.1\ \text{ohm}$ , was observed for samples prepared at the furnace temperature  $300$  and  $350\ ^\circ\text{C}$ .

The prepared Cu/Ag/Cu (IEC) sandwich samples were observed by means of both optical and electron microscopy. The presence of the compact sintered Ag layer between the copper substrates was revealed (see Fig. 3. and Fig. 4.). The microscopy methods show that the sintered Ag layer contains pores in all samples and that the size of the pores and their volume fraction depends on the temperature of sample preparation. The size of the pores and their fraction in sample prepared at  $200^\circ\text{C}$  were bigger than the pores and their fraction inside the samples prepared at higher temperatures, the nanoindentation measurement was

performed as well [10].

The electron microscopy and EDX methods have been used for studies of the all interfaces of the Cu/Ag/Cu sandwich samples. Representative photos are shown in Fig. 3. ( $200^\circ\text{C}$ ) and in Fig. 4. ( $350^\circ\text{C}$ ). The fundamental difference is the presence or absence of the copper oxide  $\text{Cu}_2\text{O}$  interlayer

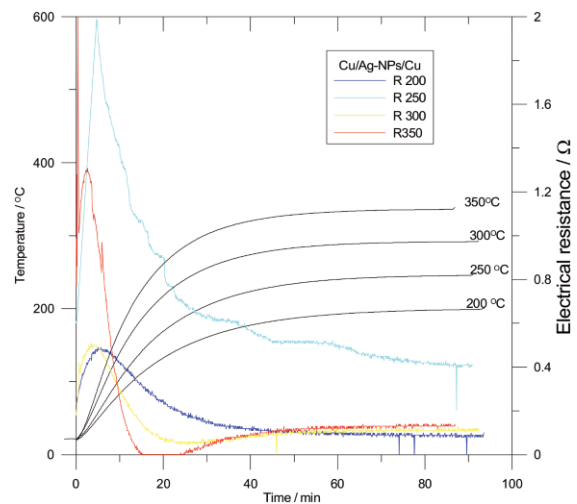


Fig. 2. The in-situ results of the temperature measurements and electrical resistance recorded during the Cu/Ag/Cu (IEC) sample preparations.

on Cu/Ag interface under air. For the sample prepared at 200°C, the oxygen content at the interface of Cu/Ag is low. For samples prepared at temperatures 250, 300, and 350°C (Fig. 4.) the occurrence of the Cu<sub>2</sub>O at the Cu/Ag interface is evident and the Cu<sub>2</sub>O layer thickness increases (at constant time of heating) with temperature of the sample preparation. For the sample prepared at 350°C (Fig. 4.) large cracks are observe on Cu/Cu<sub>2</sub>O interface. The oxygen content (Fig. 5.) respects the Cu oxidation process on Cu/Ag interface.

An important experiment is measurement of thermal effects in situ during the preparation of Cu/Ag/Cu (DSC) sandwich samples inside STA 409 calorimeter under 6N argon atmosphere. The DSC results at 10K/min rate are shown in Fig. 6. The endothermic peak can be observed with the onset of 98°C (onset of increased heat consumption for evaporation of toluene, toluene boiling point is 110°C). The

exothermic effect (maximum 175°C) can be observed within temperature range (120-200)°C. The calorimetric method enabled us to evaluate the total heat to relax during exothermic effect as (60±15) J / (1 mg Ag nanoparticles). Controlled cooling of

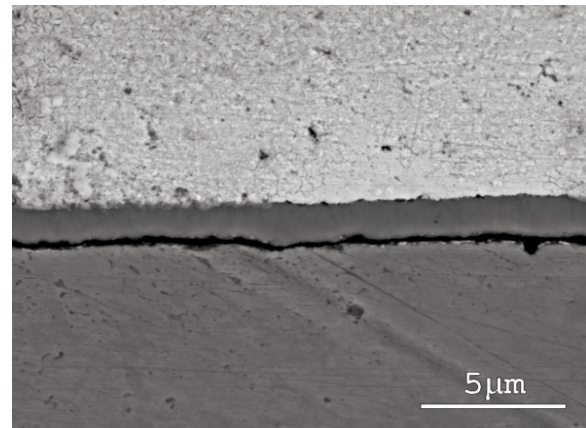


Fig. 4. SEM micrograph of the Cu/Ag/Cu (IEC) sandwich sample prepared at 350°C/1.5hrs: Cu/Ag interface cross-section. Top: sintered Ag, middle: Cu<sub>2</sub>O interlayer; dark line: crack, below: Cu substrate.

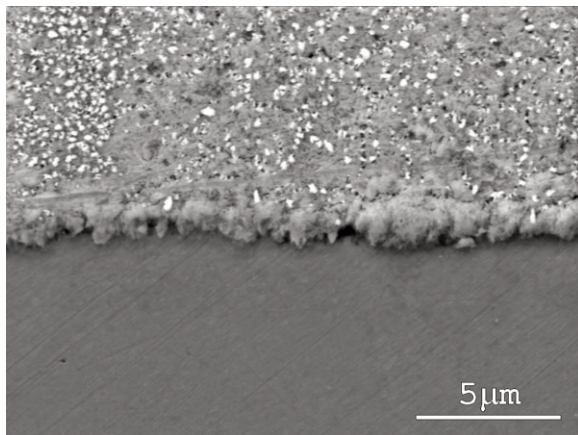


Fig. 3. SEM micrograph of the Cu/Ag/Cu (IEC) sandwich sample prepared at 200°C/1.5hrs: Cu/Ag interface cross-section. Top part: sintered Ag, bottom part: Cu substrate.

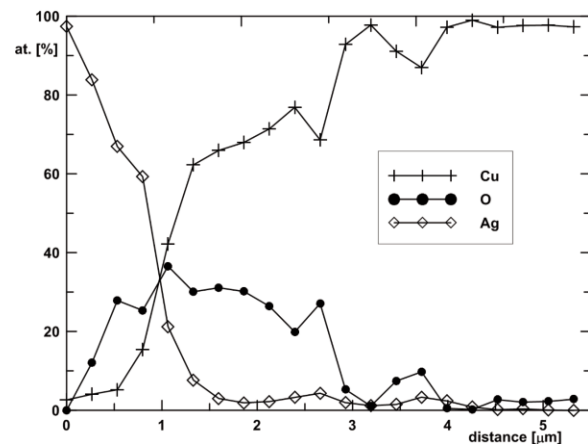


Fig. 5. EDX microanalysis series across the Ag/Cu interface of the Cu/Ag/Cu (IEC) sandwich sample prepared at 350°C/1.5hrs. Ag sintered surface at x=0.5 μm, Cu<sub>2</sub>O interlayer (0.5 to 2.5 μm), right: Cu substrate (above 2.5 μm).

Cu/Ag/Cu (DSC) sample in the calorimeter (Fig. 6.) shows no exothermic or endothermic peaks. No thermal effects within the second heat were occurred, too. The change of the argon atmosphere for synthetic air caused a big exothermal effect, which starts at approximately 200°C (see Fig. 6.).

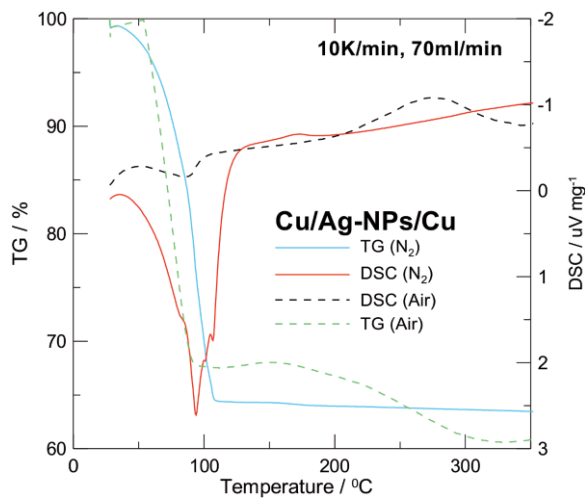


Fig. 5. The heat effects during the Cu/Ag/Cu (DSC) sandwich sample preparation inside STA409 calorimeter under inert  $N_2$  gas and synthetic air.

#### 4. Discussion

The application of the wet synthesis enables to prepare the suspension of the Ag-NPs, which can be used to join two solid copper substrates at low temperatures. An important feature of the chosen liquid phase (toluene) is to avoid oxygen transport to the suspended Ag-NPs. Another important component of the suspension is dodecyl amine, which forms an adsorbed layer (protective and stabilisation shell) on the surface of the Ag-nanoparticles. This

stabilisation layer had been created during the synthesis of the Ag nanoparticles and this layer suppresses the aggregation of the Ag-NPs. Both the liquid phase and the protective shell have an extra function to create a reducing environment, which decreases oxidation of copper substrate under air [8] at stages one and two during IEC heat treatment.

Fig. 1. shows the bimodal distribution of the Ag-NPs size. The detail of one small single Ag nanoparticle shows that the crystal lattice is uniform across particle (view along 111 direction). So on the surface of nanoparticle is not present any other phase as silver oxide layer for example.

Examination of Cu/Ag/Cu (IEC) sandwich samples reveals a consistency between the sandwich microstructure observed after sample preparation (Fig. 3. and Fig. 4.) and the in-situ measuring during their preparation (Fig. 2.). The microstructures and chemical composition profile in Fig. 5. agree also with phase diagram of Cu-Ag-O system [11]. The liquid phase (toluene) evaporation, which enables to start a destruction of the dodecyl amine protective shell, decreases the electrical resistance in the second stage of the sandwich preparation because only then Ag nanoparticles can aggregate and form the sintered Ag layer. The increase of the electrical resistance in the third stage can be explained by the fact that it forms the layer of copper oxide  $Cu_2O$ , which is a semiconductor [12, 13]. The growth of the  $Cu_2O$  layer leads to increased total electrical resistance in third stage. Cu substrate/ $Cu_2O$  incoherence and consequent formation of large cracks (see Fig. 4.) arises when  $Cu_2O$

thickness exceeds a critical value.

Cu/Ag/Cu joint creation can be understood if we look on the results of the experiment, which was carried out inside STA409 calorimeter. Here the process of the low temperature sintering of the Ag-NPs can be monitored using both thermogravimetry (TG) and DSC signal in situ. The experimental results obtained under inert gas and under synthetic air are significantly different.

Under inert gas, the TG signal starts with massive fall down, which ends at temperature of toluene boiling point. Then the TG signal remains constant. The DSC signal during first heating (see Fig. 6.) reveals a distinct endothermic peak (onset 105°C), which is caused by the evaporation of the liquid phase (toluene). When the evaporation is finished, the dodecyl amine protective shell is thermally destroyed and metallic surfaces of small Ag-NPs come into contact. The sintering (followed with exothermic heat effect) of small nanoparticles starts. The maximum heat release is at 170-175°C (see heat maxima). This is a simple mechanism how Ag nanoparticles can get rid of the surface energy. The exothermic sintering effect compensates the endothermic evaporation process at 120°C and exothermic process continues up to 210°C. The heat released during exothermic storyline from 120 to 210°C is about 60±15 J per 1g of Ag. (Note: the latent heat of melting Sn-Pb solder is -10 J per 1g of alloy).

Under synthetic air, the TG signal during first heating (see Fig. 6.) reveals again massive mass loss, which is finished at toluene boiling point. The destruction of the

dodecyl amine protective shell enables Ag-NPs oxidation (see TG mass increasing from 110-160°C). The organic protective shell is replaced by Ag oxide protective shell. The exothermal sintering effect (occurred at 110 to 200°C under inert gas) does not exist. The DSC signal starts to grow up at 200°C (heat release maxima at 275°C) but this is burning effect of organic residuals at presence of synthetic air atmosphere. The silver oxide protective shell of the Ag-NPs can be destroyed at this temperature range. Generally it is believed that decomposition temperature of bulk silver oxide in air is easy but detailed analysis of the kinetics of deoxidation of Ag in air shows that the situation may be more complicated [14]. Decomposition temperature probably also depends on the particle size of the silver oxide. Only if the Ag-NPs are free of silver oxide they can start to sinter and this process is accompanied by a decrease of the electrical resistance close to value above bulk silver resistance (see low resistance of the Cu/Ag/Cu (IEC) samples at 350°C /20min).

Under air, the Cu<sub>2</sub>O oxide interlayer between Cu substrate and sintered Ag-NPs influences the electrical resistance of the Cu/Ag/Cu joint. The lowest resistance value was achieved during in-situ experiment in the furnace preheated on 350°C at time approx 20min when the sandwich sample temperature reaches 250°C (see Fig. 2.). Later at higher temperatures, the third stage of heat treatment is observed (the electrical resistance grows up due to Cu<sub>2</sub>O oxide interlayer formation).

The protection of Ag-NPs from oxidation at low temperatures (below the sintering end

at 210°C) is important. It can be reached by a protective inert gas or by presence of protective and reducing additives in liquid phase. Otherwise, the silver oxide layer will appear. The hydrogen containing gas mixtures cannot be recommended because of safety risk and a tend to cause uncontrolled formation of metall bulk [15].

The silver oxide decomposes to Ag(s) and O<sub>2</sub>(g) elements at temperature above approx. 200-275°C. The production of the oxygen gas stabilizes the pores with internal gas overpressure and can hinder the connection. The amounts of the suspension additives have to be also carefully balanced because they lead to contamination of the sintered layer and low conductivity.

The heating rate has also an important influence on the mechanical strength of the Cu/Ag/Cu joints. Generation of vapour phase from the liquid suspension of Ag-NPs may give rise to plumes of Ag-nanoparticles and thereby impair the mechanical strength. Therefore, there is a speed limit of heating, which cannot be exceeded. Its value depends mostly on the content of Ag-NPs in suspension and on the geometry of the joints.

## 5. Conclusions

The results obtained during in-situ preparation of Cu/Ag/Cu joints allow better understanding of the processes taking place in the conductive bonding between the Cu substrate and suspension of Ag nanoparticles. It was confirmed that the preparation of joints on air at low temperature range is easier if the Ag nanoparticles suspension in the liquid phase at the presence of surfactants forming a protective layer is used.

The starting temperature of the Ag nanoparticle aggregation can be controlled by the choice of liquid phase. Using the toluene liquid phase leads to the start of aggregation and sintering process at temperature near the liquid phase boiling point. This process reveals exothermic effect ( $60 \pm 15$ ) kJ per 1g of the Ag nanoparticles. The maximum production of heat occurs at 170°C. Sintering is practically finished at 210°C.

The maximum heat generation occurs at temperatures 170°C. This temperature seems to be challenging for the preparation of the Cu/Ag/Cu electric conductive joints. Heat treatment over 275°C under air is also possible but it is accompanied by deoxidation of the Ag nanoparticles. The Cu substrate heating in air above 250°C is also associated with significant copper oxidation.

The results of the work suggest that the aggregation and sintering properties of the Ag nanoparticles and of other metal nanoparticles can be used as an alternative to lead-free soldering.

## Acknowledgement

This research was supported by the Czech Science Foundation (project 106/09/0700 and 106/09/H035), MSMT 0021622410, and Central European Institute of Technology (CEITEC MU).

## References

- [1] W.H. Qi, M.P. Wang, *Journal of Materials Science Letters*, 21 (2002) 1743.
- [2] S.L. Lai, J.Y. Guo, V. Petrova, et al., *Physical Review Letters*, 77/1 (1996) 99.



- 
- [3] Zheng B, Yamashita I, Uenuma M, et al., *Nanotechnology*, 21/4 (2010) 045305.
- [4] N.A. Luechinger, E.K. Athanassiou, W.J. Stark, *Nanotechnology*, 19/44 (2008) 445201.
- [5] J. Park, B.K. Kwak, E. Bae, et al., *J. of Nanoparticle Research*, 11/7 (2009) 1705.
- [6] H. Jiang, K.S. Moon, J. Lu, C.P. Wong, *Journal of Electronic Materials*, 34/11 (2005) 1432.
- [7] E. Ide, S. Angata, A. Hirose, et al., *Acta Materialia*, 53/8 (2005) 2385.
- [8] Angata S, Ide E, Hirose A, et al., *ASME/Pacific Rim Technical Conference on Integration and Packaging of MEMS, NEMS, and Electronic Systems*, Jul 17-22, 2005 San Francisco, p. 887.
- [9] D. Wakuda, K.S. Kim, and K. Suganua., *Scripta Materialia* 59 (2008) 649.
- [10] Charakterizace nanoindentace. nanocon Olomouc
- [11] J. Assal, B. Hallstedt, and L. J. Gauckler, *J. Phase Equilib.*, 19/4 (1998) 351.
- [12] F.C. Akkari, M. Kanzari, *Symposium on Advances in Transparent Electronics held at the 2009 EMRS Spring Meeting, JUN 08-12, 2009 Strasbourg, France* 207 (7) p. 1647
- [13] Grzesik Z, Migdalska M, Mrowec S, *Journal of physics and chemistry of solids*, 69/4 (2008) 928
- [14] G. Waterhouse, G.A. Bowmaker, J.B. Metson, *Physical Chemistry Chemical Physics*, 3/17 (2001) 3838
- [15] V. Gandova, K. Lilova, H. Malakova, B. Huber, N. Milcheva, H. Ipsler, J. Vrestal, and G. Vassilev, *J. Min. Metall. Sect. B-Metall.* 46 (1) B (2010) 11.